CONDENSED MATTER PHYSICS

Topological states from topological crystals

Zhida Song[1,2], Sheng-Jie Huang[3,4], Yang Qi[5,6,7], Chen Fang[1,8]*, Michael Hermele[3,4]*

We present a scheme to explicitly construct and classify general topological states jointly protected by an onsite symmetry group and a spatial symmetry group. We show that all these symmetry-protected topological states can be adiabatically deformed into a special class of states we call topological crystals. A topological crystal in, for example, three dimensions is a real-space assembly of finite-sized pieces of topological states in one and two dimensions protected by the local symmetry group alone, arranged in a configuration invariant under the spatial group and glued together such that there is no open edge or end. As a demonstration of principle, we explicitly enumerate all inequivalent topological crystals for noninteracting time-reversal symmetric electronic insulators with spin-orbit coupling and any one of the 230 space groups. This enumeration gives topological crystalline insulators a full classification.

INTRODUCTION

Symmetry-protected topological (SPT) phases are gapped many-body ground states that can only be adiabatically deformed into product states of local orbitals by breaking a given symmetry group or by closing the energy gap (1). Typical examples are topological insulators, topological superconductors, and the Haldane spin chain [hereinafter, if not explicitly stated otherwise, the terms "topological insulator" and "strong topological insulator" (STI) will refer to the three-dimensional (3D) topological insulator protected by time-reversal symmetry]. The best-understood SPT phases are those of noninteracting fermions; not long after the discovery of topological band insulators, free-fermion topological phases were completely classified for systems with internal (i.e., nonspatial) symmetries (2–5). Of course, crystalline symmetries play a central role in solid-state physics, so attention naturally began to turn to topological crystalline insulators (TCIs), which are electronic insulators whose topologically nontrivial nature is protected, in part, by point group or space group symmetry (5–8). Sparked by the prediction and observation of TCIs in SnTe (7, 9–11), remarkable theoretical (12–24) and experimental progress (25–27) has followed over the last few years.

Despite these developments, somewhat unexpectedly, a unified picture of the classification of noninteracting electron TCIs has yet to emerge. The primary tool for the classification of free-fermion topological phases with spatial symmetries has been K-theory (3) and equivariant K-theory (28). A number of concrete classification results have been obtained (12, 14, 16, 17, 22), but reflecting the complexity of K-theory, there is a paucity of concrete results for 3D ($d = 3$) insulators with general space group symmetry and time-reversal symmetry. Moreover, it is not understood how or whether electron interactions can be included within K-theory. Therefore, there is a need to develop alternate means to classify TCIs and other crystalline SPT (cSPT) phases jointly protected by internal and spatial symmetries. Ideally, to provide a useful complement to K-theory, these methods will be real space based and physically transparent and allow for interactions to be included.

Here, we propose a general method for classifying and constructing cSPT phases, which is then applied to the case of electronic TCIs in all 230 space groups, with time-reversal symmetry and spin-orbit coupling. We also extend these results to include STIs. Our approach is based on recent developments in the seemingly harder problem of classifying interacting cSPT phases (29–33). The key idea is to first argue that any cSPT phase is adiabatically connected to a real-space crystalline pattern of lower-dimensional topological states, which we refer to as a topological crystal (29, 32). One then develops a classification of phases of matter in terms of topological crystals. For bosonic cSPT phases with only space group symmetry, the resulting classification (32) agrees with that obtained in complementary approaches based on tensor network states and gauging crystalline symmetry (30, 31). Recently, Shiozaki et al. (34) have discussed how to formulate the topological crystal approach within K-theory via the Atiyah-Hirzebruch spectral sequence.

Our approach is related to, but goes beyond, layer constructions of TCIs. Any construction of a TCI in terms of decoupled layers, including the archetype of weak topological insulators as stacks of $d = 2$ topological insulators, is a topological crystal. However, by comparison to the recent systematic study of layer constructions in (35), we show that in certain nonsymmorphic space groups, there are TCIs that do not have a layer construction but can still be realized as topological crystals. We emphasize that all the topological states implied by symmetry eigenvalues proposed in (19, 20) are contained in our classification. The work in (35) shows that only five symmetry-eigenvalue-implied TCIs—five weak topological insulators—are not layer constructable. Here, we explicitly construct these weak topological insulators as topological crystals.

The results we obtain are related to the recent work of Khalaf et al. (36), who considered TCIs with anomalous surface states (dubbed sTCIs) and proposed a classification for sTCIs with point group and space group symmetry via the surface states of doubled STIs. The TCI classifications produced by our approach, which focuses on the bulk and does not assume anomalous surface states or a description in terms of Dirac fermions, agree with the sTCI classifications in (36). This agreement shows that all the TCIs we classify have anomalous surface states for some surface termination.

RESULTS

Topological crystals

We begin by considering a $d = 3$ system with symmetry $G = G_{\text{int}} \times G_c$, where G_{int} is some internal symmetry and G_c is either a crystalline

[1]Beijing National Research Center for Condensed Matter Physics and Institute of Physics, Chinese Academy of Sciences, Beijing 100190, China. [2]Department of Physics, Princeton University, Princeton, NJ 08544, USA. [3]Department of Physics, University of Colorado, Boulder, CO 80309, USA. [4]Center for Theory of Quantum Matter, University of Colorado, Boulder, CO 80309, USA. [5]Center for Field Theory and Particle Physics, Department of Physics, Fudan University, Shanghai 200433, China. [6]State Key Laboratory of Surface Physics, Fudan University, Shanghai 200433, China. [7]Collaborative Innovation Center of Advanced Microstructures, Nanjing 210093, China. [8]CAS Center for Excellence in Topological Quantum Computation, Beijing, China.
*Corresponding author. Email: michael.hermele@colorado.edu (M.H.); cfang@iphy.ac.cn (C.F.)

site symmetry (i.e., point group) or space group. (The assumption that G is a direct product of G_{int} and G_c is not necessary and is only made for simplicity of discussion and because it holds for the electronic TCIs to be later discussed.) We assume the system is in an SPT phase (which could be the trivial phase); that is, below an energy gap, the ground state $|\psi\rangle$ is unique and symmetry preserving, and moreover, $|\psi\rangle$ is adiabatically connected to a trivial product state if the symmetry G is broken explicitly. Moreover, we restrict to those SPT phases that only remain nontrivial in the presence of crystalline symmetry; that is, $|\psi\rangle$ is adiabatically connected to a product state if G_c is explicitly broken, even if G_{int} is preserved. To avoid complications associated with gapless boundary states, we consider periodic boundary conditions.

To proceed, we identify an asymmetric unit (AU), which is the interior of a region of space that is as large as possible, subject to the condition that no two points in the region are related by a crystalline symmetry. The AU is then copied throughout space using the crystalline symmetry, and we denote the resulting union of nonoverlapping AUs as $\mathcal{A}$. This construction gives 3D space a cell complex structure (see Methods), where the 3-cells are the individual (nonoverlapping) copies of the AU in $\mathcal{A}$. The 2-cells lie on faces where two 3-cells meet, with the property that no two distinct points in the same 2-cells are related by symmetry. Similarly, 1-cells are edges where two or more faces meet, and 0-cells are points where edges meet. The 3-cells are in one-to-one correspondence with elements of G_c: arbitrarily choosing one 3-cell to correspond to the identity element, each other 3-cell is the unique image of this one upon acting with $g \in G_c$. The 2-skeleton X^2 is the complement of $\mathcal{A}$. An example of this cell structure for the space group $P\bar{1}$ is shown in Fig. 1.

The work in (32) argued that $|\psi\rangle$ is adiabatically connected to a product of a trivial state on $\mathcal{A}$, with a possibly nontrivial state on X^2 [see section VI of (32)]. More precisely, one considers a thickened version of X^2, with characteristic thickness w, and its complement. For the argument to go through, it is important that $w \gg \xi$, where ξ is any characteristic correlation or entanglement length of the short-range entangled state $|\psi\rangle$. If G_c is a point group symmetry, then this requires no assumptions because w can be taken sufficiently large. For space group symmetry, w is limited by the unit cell size, and one must make the assumption that, by adding a fine mesh of trivial degrees of freedom, it is possible to make the correlation length ξ as small as desired. This assumption not only allows the reduction to a topological crystal state but also implies that the correlation length of the topological crystal state itself is much smaller than the unit cell size; this is important because it allows us to associate a well-defined lower-dimensional state with each cell of X^2. While we believe that this assumption is likely to hold, it is not proven, and strictly speaking, it should be treated as a conjecture. If this conjecture is false, then our approach is simply restricted to those cSPT phases whose correlation length is not bounded below upon adding trivial degrees of freedom. We note that a preliminary version of the idea of reduction to X^2 was discussed in (32); there, unlike in the present work, the idea was not developed into a tool to obtain classifications.

The result of this reduction procedure is a topological crystal state. The state on X^2 can be understood by associating a d_b-dimensional topological phase with each d_b-cell of X^2, where $d_b = 0, 1$, and 2. These lower-dimensional states are referred to as the "building blocks" of the topological crystal, and d_b is the block dimension. The building blocks must be glued together so as to eliminate any gapless modes in the bulk while preserving symmetry; for instance, $d_b = 2$ blocks will generally have gapless edge modes, which must gap out at the 1-cells and 0-cells where the building blocks meet. Whereas crystals are formed by periodically arranged atoms, i.e., zero-dimensional objects, topological crystals are "stacked" from building blocks which are themselves topological states in lower dimensions.

TCI classification

First, we note that a number of topological invariants are already known that distinguish different phases and should be a part of any classification of TCIs. In particular, these invariants include the weak $\mathbb{Z}_2$ invariants (37, 38), mirror Chern numbers ($\mathbb{Z}$ invariant) (39), and $\mathbb{Z}_2$ invariants associated with rotation (40), glide reflection (17, 18), inversion (21, 41, 42), rotoreflection (35, 36), and screw rotation (35, 36) symmetries. All possible combinations of these invariants that can be realized in TCIs with a layer construction were enumerated in (35). While one could not prove a priori that these seven quantities exhaust all independent topological invariants, in this work, we show they play a special role as a complete list of invariants for TCIs. That is, we find that any two inequivalent TCIs differ by at least one of these invariants.

To further apply the tool of topological crystals to the case of electronic TCIs, we consider a system of noninteracting electrons with spin-orbit coupling, with internal symmetries of charge conservation and time reversal; that is, $G_{protect int} = U(1) \rtimes \mathbb{Z}_2^T$. In addition, we have to specify the action of symmetry on fermionic degrees of freedom; for instance, we have Kramers time reversal T with $T^2 = (-1)^F$, where $(-1)^F$ is the fermion parity operator. More generally, some equations in the group G_c are also modified by factors of fermion parity, in a manner determined from the $d = 3$ Dirac Hamiltonian describing relativistic electrons (see the Supplementary Materials). Formally, this amounts to specifying an element $\omega_f \in H^2(G, \mathbb{Z}_2)$; we emphasize that ω_f is uniquely determined by G in the physical setting we are considering.

The next step is to understand what kind of topological crystal states can be placed on X^2. First, we consider topological crystals built out of $d = 2$ topological states. There are two kinds of 2-cells, those that coincide with a mirror plane and those that do not. 2-Cells coinciding with a mirror plane can host a $d = 2$ mirror Chern insulator (MCI) state, which is characterized by a $\mathbb{Z}$ invariant (39). The MCI state can be understood by diagonalizing the mirror operation $\sigma : z \to -z$, where z is the coordinate along the normal direction of the mirror plane. Because $\sigma^2 = (-1)^F$, one-electron wave functions can be divided into two sectors with mirror eigenvalue $\pm i$. Because $\sigma T = T\sigma$, time reversal exchanges these two sectors, which therefore have equal and opposite Chern numbers, leading to a $\mathbb{Z}$ invariant. Each sector can be understood as a $d = 2$ fermion system in class A, which has a $\mathbb{Z}$
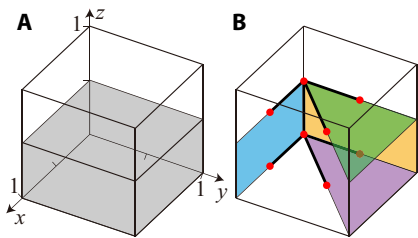

Fig. 1. Cell complex structure for space group $P\bar{1}$ (#2). (A) The AU $0 < x, y < 1$ and $0 < z < \frac{1}{2}$. (B) The symmetry-inequivalent 2-cells (colored faces), 1-cells (bold lines), and 0-cells (red dots). The other cells can be obtained from these by acting with symmetry operations.

classification. We see that the relevant symmetry class is, thus, effectively modified from AII to A on a mirror plane; this modification of symmetry class is familiar from classifications of reflection-symmetric free-fermion topological phases in momentum space (12). For 2-cells not coinciding with a mirror plane, the symmetry class remains AII, and these cells can host a $d = 2$ STI (2dTI), which is characterized by a $\mathbb{Z}_2$ invariant.

We also have to consider the possibility of topological crystals built from the $d = 1$ and $d = 0$ states. 1-Cells only host trivial states: The effective symmetry class on a 1-cell can be either AII or A (see the discussion on MCIs above), and in either case, the classification in $d = 1$ is trivial. On the other hand, there are nontrivial topological crystals built from $d_b = 0$ building blocks, which are atomic insulators formed from patterns of localized filled orbitals. Although there are distinct atomic insulators constituting different quantum phases of matter and although these distinctions may be a source of interesting physics, all these states, being product states of localized orbitals, are, in a sense, topologically trivial. Therefore, we ignore distinctions among atomic insulators in our classification. Formally, this is accomplished by taking a certain quotient (Methods). In the future, our results could be extended to include $d_b = 0$ building blocks, which would facilitate a more direct comparison with K-theory–based approaches, which do include such states.

We, thus, see that there are two kinds of TCIs, both built from $d_b = 2$ blocks. We refer to TCIs built from MCI blocks as mirror TCIs (MTCIs), while TCIs built from 2dTI blocks are dubbed $\mathbb{Z}_2$ TCIs. Of course, a general TCI can have mixed MTCI and $\mathbb{Z}_2$ TCI character, and the classification is a product of MTCI and $\mathbb{Z}_2$ TCI classifications. To proceed, we consider the requirement that the building blocks must be glued together to eliminate any gapless modes in the bulk. As shown in Methods, this requirement implies that MTCIs can always be decomposed into decoupled planar MCI layers.

$\mathbb{Z}_2$ TCIs are not quite as simple. If we consider placing a 2dTI on some subset of the 2-cells of X^2, then it can be shown these building blocks can be glued together into a topological crystal if and only if every 1-cell is the edge of an even number of 2dTI blocks (Methods). While, sometimes, these states can be decomposed into decoupled 2dTI layers, this is not always true. For example, in space group $P4_22_12$ (#94), for which the possible topological crystals are described below, we find a topological crystal that is beyond the scope of layer construction, as shown in Fig. 2B. In this state, the 2-cells decorated with 2dTIs form a complicated yet connected structure. Intuitively, one may lower the two yellow facets at $z = \frac{1}{2}$ down to $z = 0$, such that the 2dTIs form decoupled layers; however, such a process breaks the screw symmetry $\{4_{001} | \frac{1}{2}\frac{1}{2}\frac{1}{2}\}$. More rigorously, the non–layer constructability can be proved by observing that the topological invariants of this state, specifically its nontrivial weak $\mathbb{Z}_2$ invariants, cannot be obtained in any TCI constructed from decoupled 2D layers (35).

Having described TCIs in terms of topological crystals, we next use these states to classify TCIs. First, we discuss equivalence relations among topological crystal states and argue that two distinct topological crystals on X^2 are in different phases. Following (29, 32), we need to consider an additional equivalence relation, beyond those for the $d = 2$ phases of matter on the 2-cells. Within an AU and all its copies under symmetry, we create a small bubble of 2dTI and expand the bubble until it joins with the AU boundary; this process can be achieved by adiabatic evolution, preserving symmetry, within a finite time, so any two states related in this way belong to the same phase.

(Equivalently, this process can be achieved by acting with a finite depth symmetry-preserving quantum circuit.). The reason we consider a bubble of 2dTI and not something else is that this is the only nontrivial $d = 2$ state that can exist within the AU, where the only symmetries are charge conservation and time reversal. The source of this equivalence relation is the arbitrary width w of the thickened X^2 space in the dimensional reduction procedure; making w larger corresponds to bringing in additional degrees of freedom from the "bulk." However, in the present case, this equivalence operation has a trivial effect because every 2-cell is joined with two layers of 2dTI, one on each side of the 2-cell. In Methods, we give an example (without time-reversal symmetry) where this equivalence relation has a nontrivial effect.

Therefore, any two distinct topological crystal states are in different quantum phases of matter. So, to obtain a classification of TCIs, we need to enumerate possible topological crystals. First, we observe that topological crystals form an Abelian group $\mathcal{C}$ under stacking, i.e., upon superposing two different states in the same space. Because MCIs (2dTIs) are characterized by $\mathbb{Z}$ ($\mathbb{Z}_2$) invariants, $\mathcal{C}$ is a product of $\mathbb{Z}$ and $\mathbb{Z}_2$ factors, with the $\mathbb{Z}$ factors generated by MTCIs and the $\mathbb{Z}_2$ factors generated by $\mathbb{Z}_2$ TCIs. Because the MTCIs can be decomposed into decoupled planar layers, there is one $\mathbb{Z}$ factor for each symmetry-inequivalent set of mirror planes. For any particular crystalline symmetry of interest, the classification $\mathcal{C}$ is easily worked out by considering possible colorings of the faces of the AU with the MCI and 2dTI states.

To provide a concrete illustration, we here explicitly work out the topological crystals for space group $P4_22_12$. $P4_22_12$ has a tetragonal lattice and is generated from three translations $\{1 | 100\}$, $\{1 | 010\}$, and $\{1 | 001\}$, a fourfold screw $\{4_{001} | \frac{1}{2}\frac{1}{2}\frac{1}{2}\}$, and a twofold rotation $\{2_{110} | 000\}$ (here, the lattice constants are set to 1). The AU can be chosen as the region $0 < x, y, z < \frac{1}{2}$. The 2-cells and 1-cells are given, respectively, by $e_{i=1,2,3,4}^2$ and $e_{i=1,2,3,4,5,6}^1$, as shown in Fig. 2A, and their images under symmetry. There are no mirror planes, so each inequivalent 2-cell can be decorated with a 2dTI state, and possible configurations are described by four $\mathbb{Z}_2$ numbers, $n_{i = 1,2,3,4}$,
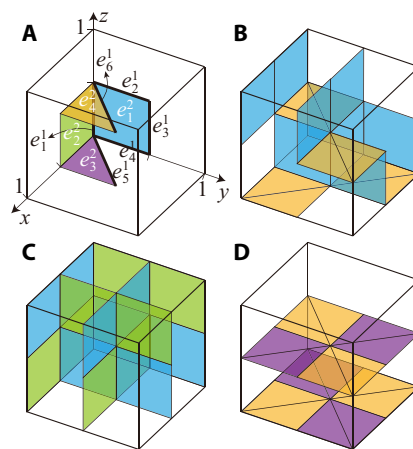
Fig. 2. Topological crystals in space group $P4_22_12$ (#94). (A) The symmetry-inequivalent 2-cells ($e_{i=1,2,3,4}^2$) and 1-cells ($e_{i=1,2,3,4,5,6}^1$) are represented by colored faces and bold lines, respectively. Here, the lattice constants are set to 1, the unit cell is given by $0 \leq x, y, z < 1$, and the AU is given by $0 < x, y, z < \frac{1}{2}$. **(B to D)** The three independent $\mathbb{Z}_2$ topological crystal generators, where only 2-cells decorated with 2dTIs are shown. **(C)** and **(D)** are layer constructions, whereas **(B)** is not.

indicating whether the corresponding e_i^2's are decorated (=1) or not (=0). The gluing condition can be expressed in matrix form

$$\sum_j A_{ij} n_j = 0 \bmod 2 \tag{1}$$

where A_{ij} is defined to be the number of 2-cells (modulo 2) that are symmetry equivalent to e_j^2, for which e_i^2 is an edge. For the setting in Fig. 2, one can immediately read out

$$A = \begin{pmatrix} 0 & 0 & 0 & 0 \\ 1 & 1 & 1 & 1 \\ 0 & 0 & 0 & 0 \\ 1 & 1 & 1 & 1 \\ 0 & 0 & 0 & 0 \\ 0 & 0 & 0 & 0 \end{pmatrix} \tag{2}$$

Solving Eq. 1, we get three independent states that generate all possible topological crystals under stacking: (i) $n_1 = n_4 = 1$, $n_2 = n_3 = 0$ (Fig. 2B); (ii) $n_1 = n_2 = 1$, $n_3 = n_4 = 0$ (Fig. 2C); and (iii) $n_3 = n_4 = 1$, $n_1 = n_2 = 0$ (Fig. 2D). While states (ii) and (iii) are obviously layer constructions, state (i) is not layer constructible, as discussed above.

Topological invariants

Now, we turn to the topological invariants characterizing topological crystals. First, all MTCIs are characterized by real-space Chern numbers associated with certain mirror planes, and the mirror Chern numbers in momentum space for each of them are listed in (35). Therefore, we focus on $\mathbb{Z}_2$ TCIs. Given a $\mathbb{Z}_2$ TCI and its corresponding topological crystal, for each symmetry operation $g \in G_c$, we assign a $\mathbb{Z}_2$ number $\delta(g)$. We arbitrarily choose one AU and let $\mathbf{r}$ be a point inside, then we set $\delta(g) = 1$ [$\delta(g) = 0$] if a path connecting $\mathbf{r}$ to $g\mathbf{r}$ crosses through an odd (even) number of 2dTI 2-cells. It is shown in Methods that (1) $\delta(g)$ is well defined, independent of the arbitrary choices of AU, $\mathbf{r}$, and the path connecting $\mathbf{r}$ to $g\mathbf{r}$, and (2) $\delta(g_1 g_2) = \delta(g_1) + \delta(g_2)$. The latter property implies that δ is a homomorphism from G_c to $\mathbb{Z}_2$ [or, equivalently, an element of $H^1(G_c, \mathbb{Z}_2)$], which means that it is enough to specify $\delta(g)$ for the generators of G_c. $\delta(g)$ encodes all the $\mathbb{Z}_2$ invariants for TCIs listed earlier, by choosing different operations g. For instance, if g is a translation, then $\delta(g)$ is the corresponding $\mathbb{Z}_2$ weak invariant, if g is inversion, then $\delta(g)$ is the $\mathbb{Z}_2$ inversion invariant, and so on.

As an example, the topological crystal shown in Fig. 2B has $\delta(\{1 \,|\, 100\}) = 0$, $\delta(\{1 \,|\, 010\}) = 0$, $\delta(\{1 \,|\, 001\}) = 1$, $\delta(\{4_{001} \,|\, \frac{1}{2}\frac{1}{2}\frac{1}{2}\}) = 0$, and $\delta(\{2_{110} \,|\, 000\}) = 0$. Taking advantage of the results in (35), we find that these invariants, together with the mirror Chern number, uniquely label all the TCIs in our classification, and moreover, we find all TCIs that are beyond layer construction by comparing with (35) (Supplementary Materials).

As suggested by the above discussion of invariants, the classification $\mathcal{C}$ of TCIs has a simple relationship with $H^1(G_c, \mathbb{Z}_2)$, which allows us to efficiently compute $\mathcal{C}$ and obtain the full TCI classification $\mathcal{C}$ for all space groups (Methods); the results are given in Table 2.

Moreover, we find that there are 12 groups hosting topological crystals beyond layer construction (Fig. 3); for these non–layer-constructable states, we tabulated their invariants and symmetry-based indicators (19, 20) in the Supplementary Materials, completing the

mapping from indicators to TCI invariants (35). Table 1 gives the classification of TCIs protected by point group symmetry for the 32 crystallographic point groups in three dimensions.

Last, given the classification of TCIs, we obtained simple rules that extend this classification to include STIs. The key fact is that upon stacking two identical STIs together, one can either obtain a trivial state or a nontrivial TCI. Upon identifying the state thus obtained, we obtain a full classification of all topologically nontrivial insulators of noninteracting electrons with time-reversal symmetry and spin-orbit coupling.

Unified classification of STIs and TCIs

We have focused thus far on classifying TCIs, where crystalline symmetry is required to protect a nontrivial cSPT phase. Here, we address a more general problem, namely, the classification of all $d = 3$ free-electron insulators with time-reversal symmetry, spin-orbit coupling, and arbitrary crystalline point group or space group symmetry. We still ignore distinctions among atomic insulators, so the one new state that must be added as a generator of the classification is the STI, which is, of course, robust even upon breaking crystalline symmetry.

First, we assume that the STI is compatible with an arbitrary crystalline symmetry. We expect that this is true, but to our knowledge, it has not been proved rigorously. One argument in favor of this expectation is to note that the STI can be described by a continuum theory of a massive Dirac fermion, which is invariant under arbitrary rigid motions of 3D space. This symmetry can be broken down to an arbitrary space group or point group symmetry, for instance, by adding a periodic potential, which produces a model of an STI with arbitrary space group symmetry. This is not quite a rigorous argument because one has to show that it is possible to regularize the continuum theory in a manner compatible with an arbitrary lattice symmetry. Another argument is to note that any centrosymmetric space group has a $\mathbb{Z}_4$ indicator (20), and according to the Fu-Kane formula (37), the root state with $z_4 = 1$ is an STI. While it was argued that any symmetry indicator can be realized by a band structure, there is no guarantee that the resulting band structure is an insulator (20). Assuming an STI can indeed be found for each centrosymmetric space group, then we need only note that every noncentrosymmetric space group is a subgroup of some centrosymmetric space group, so an STI compatible with the latter is compatible with the former. To show this expectation holds rigorously, a straightforward approach would be to find a small number of space groups that contain all space groups as subgroups and exhibit a model realizing an STI for each of these symmetry groups.

Next, we would like to compute the classification $\mathcal{C}_{\text{full}}$ including both TCIs and STIs. The topological crystal picture tells us that TCIs are a subgroup (i.e., $\mathcal{C} \subset \mathcal{C}_{\text{full}}$) because stacking two TCIs produces another TCI or a trivial state. It is also true that $\mathcal{C}_{\text{full}}/\mathcal{C} \simeq \mathbb{Z}_2$, because this quotient corresponds to ignoring the distinctions among TCIs, which leaves only a $\mathbb{Z}_2$ generated by the STI. It follows that $|C_{\text{full}}| = 2\,|\mathcal{C}|$ when the TCI classification is finite. One might expect $\mathcal{C}_{\text{full}} = \mathcal{C} \times \mathbb{Z}_2$, with the $\mathbb{Z}_2$ factor generated by the STI, but this is not true in general because stacking two identical STIs can result in a nontrivial TCI. Put another way, $\mathcal{C}_{\text{full}}$ can be a nontrivial group extension of $\mathcal{C}$ by $\mathbb{Z}_2$, and we need to solve this group extension problem.

We proceed by choosing a particular STI state and stacking this state with itself to get a state we call $(\text{STI})^2$. We know that $(\text{STI})^2$ has trivial strong index and is, thus, either a nontrivial TCI or a trivial state, that is, $(\text{STI})^2 \in \mathcal{C}$. We need to determine the element of $\mathcal{C}$ given

Table 1. Classifications $\mathcal{C}$ of TCIs for noninteracting electrons with time-reversal symmetry, spin-orbit coupling, and crystalline point group symmetry. N/A denotes a trivial classification. Full classifications including strong topological insulators can be easily obtained from this table by using the group extension rules given in Results and are also provided as a table in the Supplementary Materials.

Point group	TCI classification
1	N/A
$\bar{1}$	$\mathbb{Z}_2$
2	$\mathbb{Z}_2$
m	$\mathbb{Z}$
$2/m$	$\mathbb{Z} \times \mathbb{Z}_2$
222	$\mathbb{Z}_2^2$
$mm2$	$\mathbb{Z}^2$
mmm	$\mathbb{Z}^3$
4	$\mathbb{Z}_2$
$\bar{4}$	$\mathbb{Z}_2$
$4/m$	$\mathbb{Z} \times \mathbb{Z}_2$
422	$\mathbb{Z}_2^2$
$4mm$	$\mathbb{Z}^2$
$\bar{4}2m$	$\mathbb{Z} \times \mathbb{Z}_2$
$4/mmm$	$\mathbb{Z}^3$
3	N/A
$\bar{3}$	$\mathbb{Z}_2$
32	$\mathbb{Z}_2$
$3m$	$\mathbb{Z}$
$\bar{3}m$	$\mathbb{Z} \times \mathbb{Z}_2$
6	$\mathbb{Z}_2$
$\bar{6}$	$\mathbb{Z}$
$6/m$	$\mathbb{Z} \times \mathbb{Z}_2$
622	$\mathbb{Z}_2^2$
$6mm$	$\mathbb{Z}^2$
$\bar{6}2m$	$\mathbb{Z}^2$
$6/mmm$	$\mathbb{Z}^3$
23	N/A
$m3$	$\mathbb{Z}$
432	$\mathbb{Z}_2$
$\bar{4}3m$	$\mathbb{Z}$
$m\bar{3}m$	$\mathbb{Z}^2$

by $(\text{STI})^2$. First, we observe that our choice of STI is arbitrary under stacking with a TCI because this stacking does not change the strong invariant. It is obvious that stacking STI with a $\mathbb{Z}_2$ TCI does not affect $(\text{STI})^2$, but stacking STI with an MTCI can change the $\mathbb{Z}$ invariants of $(\text{STI})^2$ by arbitrary even integers, depending on the choice of MTCI. We, thus, see that the information in $(\text{STI})^2$ that is independent of the arbitrary choice of STI is precisely the information preserved under the map $\pi : \mathcal{C} \rightarrow \tilde{\mathcal{C}} \simeq H^1(G_c, \mathbb{Z}_2)$ introduced in Methods. Therefore, $(\text{STI})^2$ is characterized by a homomorphism from $G_c \rightarrow \mathbb{Z}_2$, namely, $\pi((\text{STI})^2) \in H^1(G_c, \mathbb{Z}_2)$. Determining $\pi((\text{STI})^2)$ solves the group extension problem and determines the group $\mathcal{C}_{\text{full}}$.

Denoting the homomorphism given by $\pi((\text{STI})^2)$ by $\delta : G_c \rightarrow \mathbb{Z}_2$, it is natural to conjecture that $\delta(g) = 0$ when g is a rigid motion preserving the orientation of space (e.g., translations and rotations), and $\delta(g) = 1$ when g reverses orientation (e.g., inversion, reflections, and glide reflections). This conjecture is natural because the map δ should depend only on the crystalline symmetry G_c, and there does not seem to be any other nontrivial map that can be defined in a uniform way for all G_c.

We can establish this conjecture using results of Khalaf *et al.* (*36*), where the authors studied surface theories obtained by stacking two STIs. For a crystalline symmetry G_c^{surf} preserved by some surface termination, they considered a mass texture on the boundary satisfying $m_{g\mathbf{r}} = s_g m_{\mathbf{r}}$, where $g \in G_c^{\text{surf}}$, $\mathbf{r}$ is a point on the boundary, $m_{\mathbf{r}}$ is the Dirac mass, and $s_g = \pm 1$ keeps track of sign changes in the mass. They showed that $s_{g_1 g_2} = s_{g_1} s_{g_2}$, i.e., s_g defines a homomorphism from G_c^{surf} to $\mathbb{Z}_2$. Moreover, they showed that, in the case of stacking two identical STIs, $s_g = \det R_g$ (this result follows from equation 14 of (*36*) upon taking $\eta_g^{(1)} = \eta_g^{(2)}$, as appropriate for identical STIs). Here, g is the rigid motion $\{R_g | \mathbf{t}_g\}$, where R_g is an O(3) matrix and $\mathbf{t}_g$ is a translation vector. Because $\det R_g = 1$ ($\det R_g = -1$) for orientation-preserving (orientation-reversing) operations, this result is identical to our conjecture upon identifying that $s_g = (-1)^{\delta(g)}$. Physically, s_g and $\delta(g)$ should be, thus, identified because the gapless lines on the surface where the mass changes sign are, in the topological crystal picture, precisely the gapless edges of 2-cells touching the surface.

The argument is not quite complete because the crystalline symmetry G_c cannot generally be preserved by a surface termination. However, we found that specifying the seven types of invariants listed in the Results section uniquely determines a TCI phase (element of $\mathcal{C}$). Therefore, we can take G_c^{surf} to be the subgroup of G_c associated with each invariant. It is always possible to choose a surface termination preserving such G_c^{surf}, so we can run the above argument for each such subgroup. This then determines $\pi((\text{STI})^2)$.

This result determines the group structure of $\mathcal{C}_{\text{full}}$. There are three cases: (i) If G_c contains only orientation-preserving operations, then $\mathcal{C}_{\text{full}} = \mathcal{C} \times \mathbb{Z}_2$. (ii) If G_c contains orientation-reversing operations but no mirror reflections, and hence $\mathcal{C}$ has no $\mathbb{Z}$ factors, then one of the $\mathbb{Z}_2$ factors in $\mathcal{C}$ is replaced in $\mathcal{C}_{\text{full}}$ by a $\mathbb{Z}_4$ factor. (iii) If G_c contains mirror reflections, then $(\text{STI})^2$ generates a $\mathbb{Z}$ factor in $\mathcal{C}$. In this case, $\mathcal{C}_{\text{full}}$ and $\mathcal{C}$ have the same group structure, but in $\mathcal{C}_{\text{full}}$, the generator of one of the $\mathbb{Z}$ factors is an STI state. These rules easily allow one to obtain $\mathcal{C}_{\text{full}}$ for all the crystallographic point groups and space groups, and the results are given as tables in the Supplementary Materials. Because $\pi((\text{STI})^2)$ is known, it is also straightforward to explicitly construct the topological crystal corresponding to $(\text{STI})^2$, up to the arbitrariness in defining STI. We note that recently, (*43*) used K-theory to obtain classifications for crystallographic point
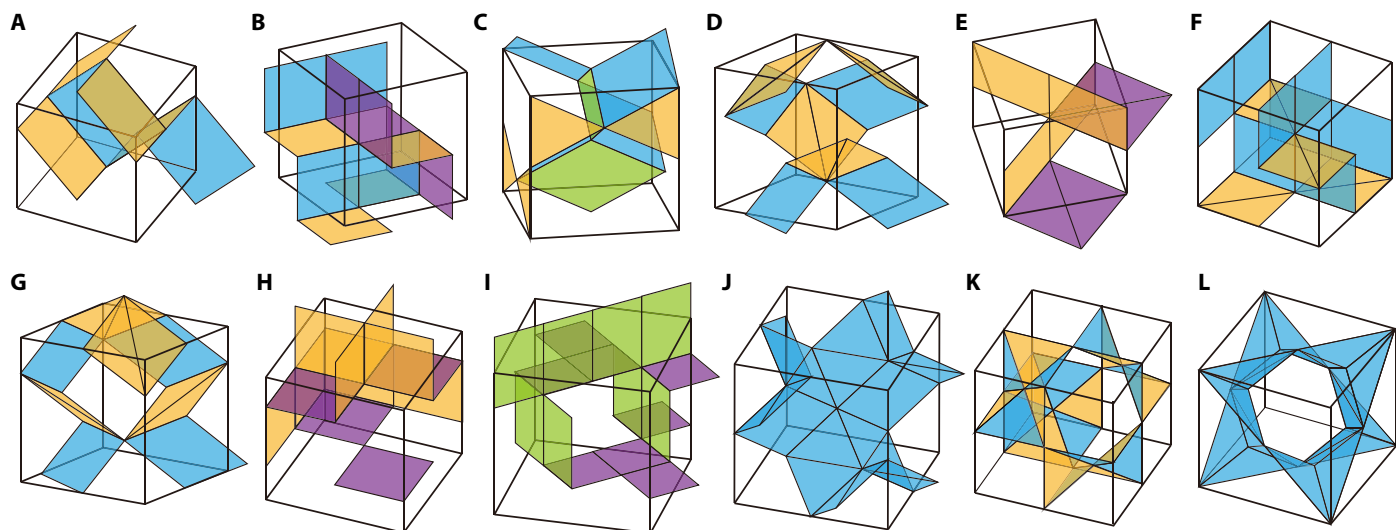
Fig. 3. Illustrations of the topological crystals beyond layer construction. (**A**) to (**L**) show these states for space groups *Pnn*2 (#34), *Pnnn* (#48), *P*4$_2$ (#77), *P*4$_2$/*n* (#86), *P*4$_2$22 (#93), *P*4$_2$2$_1$2 (#94), *P*4$_2$*cm* (#102), *P*$\overline{4}$*n*2 (#118), *P*4$_2$/*nnm* (#134), *Pn*$\overline{3}$ (#201), *P*4$_3$32 (#208), and *Pn*$\overline{3}$*m* (#224), respectively. Inequivalent 2-cells are represented by different colors. The topological invariants of these topological crystals and the coordinates of the plotted 2-cells can be found in the Supplementary Materials.

groups in $d = 3$. To compare these results with ours for all point groups would, for instance, require extending our results to include topological crystals with $d_b = 0$ bulding blocks. However, for the nine nontrivial point groups where all operations share a common fixed line or fixed plane (C_n, C_s, and C_{nv}), states with $d_b = 0$ building blocks are not relevant, and for these point groups, our results agree with those of (*43*).

DISCUSSION

Our method provides a unified, real-space perspective for TCIs, complementary to the momentum-space perspective usually taken for free-fermion systems. Real-space constructions have an advantage when electron interactions are considered. For example, because all $\mathbb{Z}_2$ TCIs are made from 2dTIs, from the stability of the 2dTI phase against interactions, we immediately know that the classification of $\mathbb{Z}_2$ TCIs is not affected by interactions. On the other hand, the $\mathbb{Z}$ classification of $d = 2$ MCI states collapses to $\mathbb{Z}_8$ in the presence of interactions (*44*). This implies that the classification of MTCIs does collapse, but the $\mathbb{Z}$ invariants characterizing MTCIs are robust to interactions modulo 8.

One can easily use the idea of topological crystals to classify free-electron $d = 3$ insulators with time-reversal but without spin-orbit coupling, that is, with SU(2) spin rotation symmetry. For these systems, time reversal and crystalline symmetry can be taken to act trivially on electron operators, with no factors of fermion parity, and in particular $T^2 = 1$. It can then be seen that all 2-cells have symmetry class AI, while 1-cells can be in class AI or A. In all these cases, only trivial states are possible, and no free-electron TCIs can occur. This means that any nonzero symmetry-based indicator implies some topological nodes in the bulk, proved by exhaustion in (*45*).

The topological crystal approach developed here can be applied in many other physical settings. For instance, one can classify topological crystalline superconductors, described at the free-fermion level by Bogoliubov–de Gennes Hamiltonians. Moreover, as other works have begun to explore, it is also possible to use topological crystals to classify interacting fermionic cSPT phases.

METHODS
Cell complex structure
A cell complex is a topological space constructed by gluing together points (0-cells) and n-dimensional balls (n-cells). In more detail, to construct a cell complex X, one starts with a set of discrete points X^0, referred to as the 0-skeleton. Next, one forms the 1-skeleton X^1 by attaching a set of 1-cells to X^0. To attach a 1-cell, one starts with a closed interval on the real line (whose interior is the 1-cell), and the two endpoints are identified with points in X^0. The resulting space X^1 is given by attaching the 1-cells to X^0. The process continues in the natural way; for instance, to attach a 2-cell to X^1, we start with a 2D disc D with boundary (whose interior is the 2-cell) and identify ∂D with a subset of X^1 using a continuous map from ∂D to X^1. The n-skeleton X^n is given by attaching the n-cells to X^{n-1}. A more detailed discussion can be found in the book by Hatcher (*46*).

Here, we describe in more detail how 3D space $\mathbb{R}^3$ can be given a cell complex structure upon choosing an AU. An AU is an open sub-set of $\mathbb{R}^3$ that is as large as possible, subject to the condition that no two points in the AU are related by the action of G_c. The choice of AU is not unique. While not strictly necessary, we can always choose an AU such that the boundary of the closure of the AU consists of segments of flat planes; that is, in the case of space group symmetry, the AU can be chosen as the interior of a polyhedron. Once we choose an AU, it and its copies under the action of G_c form the 3-cells, which are in one-to-one correspondence with the elements of G_c. The union of all the 3-cells is denoted by $\mathcal{A}$, and its complement $X^2 = \mathbb{R}^3 - \mathcal{A}$ is the 2-skeleton of the cell complex.

We choose 2-cells of X^2 satisfying three properties: (1) Each 2-cell is a subset of a face where two 3-cells meet. To be precise, we say that two 3-cells meet at a face when the intersection of their closures is

Table 2. TCI classifications C for noninteracting electrons with time-reversal symmetry and spin-orbit coupling, given for all space groups. N/A denotes a trivial classification. Full classifications including strong topological insulators can be easily obtained from this table by using the group extension rules given in Results and are also provided as a table in the Supplementary Materials.

1	$\mathbb{Z}_2^3$	41	$\mathbb{Z}_2^3$	81	$\mathbb{Z}_2^3$	121	$\mathbb{Z}\times\mathbb{Z}_2^2$	161	$\mathbb{Z}_2$	201	$\mathbb{Z}_2^2$
2	$\mathbb{Z}_2^4$	42	$\mathbb{Z}^2\times\mathbb{Z}_2^2$	82	$\mathbb{Z}_2^2$	122	$\mathbb{Z}_2^2$	162	$\mathbb{Z}\times\mathbb{Z}_2^2$	202	$\mathbb{Z}$
3	$\mathbb{Z}_2^4$	43	$\mathbb{Z}_2^2$	83	$\mathbb{Z}^2\times\mathbb{Z}_2^2$	123	$\mathbb{Z}^5$	163	$\mathbb{Z}_2^2$	203	$\mathbb{Z}_2$
4	$\mathbb{Z}_2^3$	44	$\mathbb{Z}^2\times\mathbb{Z}_2$	84	$\mathbb{Z}\times\mathbb{Z}_2^2$	124	$\mathbb{Z}\times\mathbb{Z}_2^3$	164	$\mathbb{Z}\times\mathbb{Z}_2^2$	204	$\mathbb{Z}\times\mathbb{Z}_2$
5	$\mathbb{Z}_2^3$	45	$\mathbb{Z}_2^3$	85	$\mathbb{Z}_2^3$	125	$\mathbb{Z}\times\mathbb{Z}_2^3$	165	$\mathbb{Z}_2^2$	205	$\mathbb{Z}_2$
6	$\mathbb{Z}^2\times\mathbb{Z}_2^2$	46	$\mathbb{Z}\times\mathbb{Z}_2^2$	86	$\mathbb{Z}_2^3$	126	$\mathbb{Z}_2^3$	166	$\mathbb{Z}\times\mathbb{Z}_2^2$	206	$\mathbb{Z}_2^2$
7	$\mathbb{Z}_2^3$	47	$\mathbb{Z}^6$	87	$\mathbb{Z}\times\mathbb{Z}_2^2$	127	$\mathbb{Z}^3\times\mathbb{Z}_2$	167	$\mathbb{Z}_2^2$	207	$\mathbb{Z}_2^2$
8	$\mathbb{Z}\times\mathbb{Z}_2^2$	48	$\mathbb{Z}_2^4$	88	$\mathbb{Z}_2^2$	128	$\mathbb{Z}\times\mathbb{Z}_2^2$	168	$\mathbb{Z}_2^2$	208	$\mathbb{Z}_2^2$
9	$\mathbb{Z}_2^2$	49	$\mathbb{Z}\times\mathbb{Z}_2^4$	89	$\mathbb{Z}_2^4$	129	$\mathbb{Z}^2\times\mathbb{Z}_2^2$	169	$\mathbb{Z}_2$	209	$\mathbb{Z}_2$
10	$\mathbb{Z}^2\times\mathbb{Z}_2^3$	50	$\mathbb{Z}_2^4$	90	$\mathbb{Z}_2^3$	130	$\mathbb{Z}_2^3$	170	$\mathbb{Z}_2$	210	$\mathbb{Z}_2$
11	$\mathbb{Z}\times\mathbb{Z}_2^3$	51	$\mathbb{Z}^3\times\mathbb{Z}_2^2$	91	$\mathbb{Z}_2^3$	131	$\mathbb{Z}^3\times\mathbb{Z}_2$	171	$\mathbb{Z}_2^2$	211	$\mathbb{Z}_2^2$
12	$\mathbb{Z}\times\mathbb{Z}_2^3$	52	$\mathbb{Z}_2^3$	92	$\mathbb{Z}_2^2$	132	$\mathbb{Z}^2\times\mathbb{Z}_2^2$	172	$\mathbb{Z}_2^2$	212	$\mathbb{Z}_2$
13	$\mathbb{Z}_2^4$	53	$\mathbb{Z}\times\mathbb{Z}_2^3$	93	$\mathbb{Z}_2^4$	133	$\mathbb{Z}_2^3$	173	$\mathbb{Z}_2$	213	$\mathbb{Z}_2$
14	$\mathbb{Z}_2^3$	54	$\mathbb{Z}_2^4$	94	$\mathbb{Z}_2^3$	134	$\mathbb{Z}\times\mathbb{Z}_2^3$	174	$\mathbb{Z}^2$	214	$\mathbb{Z}_2^2$
15	$\mathbb{Z}_2^3$	55	$\mathbb{Z}^2\times\mathbb{Z}_2^2$	95	$\mathbb{Z}_2^3$	135	$\mathbb{Z}\times\mathbb{Z}_2^2$	175	$\mathbb{Z}^2\times\mathbb{Z}_2$	215	$\mathbb{Z}\times\mathbb{Z}_2$
16	$\mathbb{Z}_2^5$	56	$\mathbb{Z}_2^3$	96	$\mathbb{Z}_2^2$	136	$\mathbb{Z}^2\times\mathbb{Z}_2$	176	$\mathbb{Z}\times\mathbb{Z}_2$	216	$\mathbb{Z}$
17	$\mathbb{Z}_2^4$	57	$\mathbb{Z}\times\mathbb{Z}_2^3$	97	$\mathbb{Z}_2^3$	137	$\mathbb{Z}\times\mathbb{Z}_2^2$	177	$\mathbb{Z}_2^3$	217	$\mathbb{Z}\times\mathbb{Z}_2$
18	$\mathbb{Z}_2^3$	58	$\mathbb{Z}\times\mathbb{Z}_2^2$	98	$\mathbb{Z}_2^3$	138	$\mathbb{Z}\times\mathbb{Z}_2^2$	178	$\mathbb{Z}_2^2$	218	$\mathbb{Z}_2$
19	$\mathbb{Z}_2^2$	59	$\mathbb{Z}^2\times\mathbb{Z}_2^2$	99	$\mathbb{Z}^3\times\mathbb{Z}_2$	139	$\mathbb{Z}^3\times\mathbb{Z}_2$	179	$\mathbb{Z}_2^2$	219	$\mathbb{Z}_2$
20	$\mathbb{Z}_2^3$	60	$\mathbb{Z}_2^3$	100	$\mathbb{Z}\times\mathbb{Z}_2^2$	140	$\mathbb{Z}^2\times\mathbb{Z}_2^2$	180	$\mathbb{Z}_2^3$	220	$\mathbb{Z}_2$
21	$\mathbb{Z}_2^4$	61	$\mathbb{Z}_2^3$	101	$\mathbb{Z}\times\mathbb{Z}_2^2$	141	$\mathbb{Z}\times\mathbb{Z}_2^2$	181	$\mathbb{Z}_2^3$	221	$\mathbb{Z}^3$
22	$\mathbb{Z}_2^4$	62	$\mathbb{Z}\times\mathbb{Z}_2^2$	102	$\mathbb{Z}\times\mathbb{Z}_2^2$	142	$\mathbb{Z}_2^3$	182	$\mathbb{Z}_2^2$	222	$\mathbb{Z}_2^2$
23	$\mathbb{Z}_2^3$	63	$\mathbb{Z}^2\times\mathbb{Z}_2^2$	103	$\mathbb{Z}_2^3$	143	$\mathbb{Z}_2$	183	$\mathbb{Z}^2\times\mathbb{Z}_2$	223	$\mathbb{Z}\times\mathbb{Z}_2$
24	$\mathbb{Z}_2^3$	64	$\mathbb{Z}\times\mathbb{Z}_2^3$	104	$\mathbb{Z}_2^2$	144	$\mathbb{Z}_2$	184	$\mathbb{Z}_2^2$	224	$\mathbb{Z}\times\mathbb{Z}_2^2$
25	$\mathbb{Z}^4\times\mathbb{Z}_2$	65	$\mathbb{Z}^4\times\mathbb{Z}_2$	105	$\mathbb{Z}^2\times\mathbb{Z}_2$	145	$\mathbb{Z}_2$	185	$\mathbb{Z}\times\mathbb{Z}_2$	225	$\mathbb{Z}^2$
26	$\mathbb{Z}^2\times\mathbb{Z}_2^2$	66	$\mathbb{Z}\times\mathbb{Z}_2^3$	106	$\mathbb{Z}_2^2$	146	$\mathbb{Z}_2$	186	$\mathbb{Z}\times\mathbb{Z}_2$	226	$\mathbb{Z}\times\mathbb{Z}_2$
27	$\mathbb{Z}_2^4$	67	$\mathbb{Z}^2\times\mathbb{Z}_2^3$	107	$\mathbb{Z}^2\times\mathbb{Z}_2$	147	$\mathbb{Z}_2^2$	187	$\mathbb{Z}^3$	227	$\mathbb{Z}\times\mathbb{Z}_2$
28	$\mathbb{Z}\times\mathbb{Z}_2^3$	68	$\mathbb{Z}_2^4$	108	$\mathbb{Z}\times\mathbb{Z}_2^2$	148	$\mathbb{Z}_2^2$	188	$\mathbb{Z}\times\mathbb{Z}_2$	228	$\mathbb{Z}_2^2$
29	$\mathbb{Z}_2^3$	69	$\mathbb{Z}^3\times\mathbb{Z}_2^2$	109	$\mathbb{Z}\times\mathbb{Z}_2$	149	$\mathbb{Z}_2^2$	189	$\mathbb{Z}^3$	229	$\mathbb{Z}^2\times\mathbb{Z}_2$
30	$\mathbb{Z}_2^3$	70	$\mathbb{Z}_2^3$	110	$\mathbb{Z}_2^2$	150	$\mathbb{Z}_2^2$	190	$\mathbb{Z}\times\mathbb{Z}_2$	230	$\mathbb{Z}_2^2$
31	$\mathbb{Z}\times\mathbb{Z}_2^2$	71	$\mathbb{Z}^3\times\mathbb{Z}_2$	111	$\mathbb{Z}\times\mathbb{Z}_2^3$	151	$\mathbb{Z}_2^2$	191	$\mathbb{Z}^4$		
32	$\mathbb{Z}_2^3$	72	$\mathbb{Z}\times\mathbb{Z}_2^3$	112	$\mathbb{Z}_2^3$	152	$\mathbb{Z}_2^2$	192	$\mathbb{Z}\times\mathbb{Z}_2^2$		
33	$\mathbb{Z}_2^2$	73	$\mathbb{Z}_2^4$	113	$\mathbb{Z}\times\mathbb{Z}_2^2$	153	$\mathbb{Z}_2^2$	193	$\mathbb{Z}^2\times\mathbb{Z}_2$		
34	$\mathbb{Z}_2^3$	74	$\mathbb{Z}^2\times\mathbb{Z}_2^2$	114	$\mathbb{Z}_2^2$	154	$\mathbb{Z}_2^2$	194	$\mathbb{Z}^2\times\mathbb{Z}_2$		
35	$\mathbb{Z}^2\times\mathbb{Z}_2^2$	75	$\mathbb{Z}_2^3$	115	$\mathbb{Z}^2\times\mathbb{Z}_2^2$	155	$\mathbb{Z}_2^2$	195	$\mathbb{Z}_2$		

continued on next page

36	$\mathbb{Z} \times \mathbb{Z}_2^2$	76	$\mathbb{Z}_2^2$	116	$\mathbb{Z}_2^3$	156	$\mathbb{Z} \times \mathbb{Z}_2$	196	N/A
37	$\mathbb{Z}_2^3$	77	$\mathbb{Z}_2^3$	117	$\mathbb{Z}_2^3$	157	$\mathbb{Z} \times \mathbb{Z}_2$	197	$\mathbb{Z}_2$
38	$\mathbb{Z}^3 \times \mathbb{Z}_2$	78	$\mathbb{Z}_2^3$	118	$\mathbb{Z}_2^3$	158	$\mathbb{Z}_2$	198	N/A
39	$\mathbb{Z} \times \mathbb{Z}_2^3$	79	$\mathbb{Z}_2^3$	119	$\mathbb{Z} \times \mathbb{Z}_2^2$	159	$\mathbb{Z}_2$	199	$\mathbb{Z}_2$
40	$\mathbb{Z} \times \mathbb{Z}_2^3$	80	$\mathbb{Z}_2^2$	120	$\mathbb{Z}_2^3$	160	$\mathbb{Z} \times \mathbb{Z}_2$	200	$\mathbb{Z}^2$

homeomorphic to a 2-manifold (possibly with boundary), and we define the face where they meet to be this intersection. (2) No two distinct points in the same 2-cell are related under the action of G_c. Note that a 2-cell may be a subset of a mirror plane, in which case the mirror symmetry will take every point in the 2-cell to itself. This property ensures that each 2-cell has no spatial symmetries; if there is a mirror symmetry, it acts on the 2-cell effectively as an internal symmetry. (3) The 2-cell structure on X^2 respects the G_c symmetry. Precisely, given a 2-cell e^2 and a symmetry operation $g \in G_c$, the image $g(e^2)$ is also a 2-cell.

It is always possible to choose a set of 2-cells satisfying these properties: We started with the set of faces where pairs of 3-cells meet and took their interiors as 2-manifolds. This gives a set of 2-cells for X^2 satisfying properties (1) and (3), but property (2) need not be satisfied. This can be rectified by dividing up the 2-cells until property (2) is satisfied.

Letting $\mathcal{A}_2$ be the union of all the 2-cells, the 1-skeleton X^1 is $X^2 - \mathcal{A}_2$. We choose 1-cells to satisfy three properties very similar to those for 2-cells. A difference from the 2-cell case is that different numbers of 2-cells can meet at a 1-cell; we would like to ensure that the same set of n 2-cells meets everywhere along the extent of a given 1-cell. We therefore modified property (1) as follows: Each 1-cell is a subset of an edge where exactly n 2-cells meet. More precisely, we say that n 2-cells meet at an edge when the intersection of their closures is homeomorphic to a 1-manifold (possibly with boundary), and the edge where they meet is defined to be this intersection. Apart from these n 2-cells, we require the edge to have empty intersection with the closure of any other 2-cell. Properties (2) and (3) are required to hold with the obvious modifications.

The 0-cells are just the points where two or more 1-cells meet. Formally, letting $\mathcal{A}_1$ be the union of all 1-cells, the 0-cells are the points of $X^1 - \mathcal{A}_1$.

We illustrate this rather abstract discussion with some examples. First, we considered $G_c = C_i$, the point group generated by inversion symmetry. We took the AU to be the half space $z > 0$, and the 3-cells are then the two half-spaces $z > 0$ and $z < 0$. There are two 2-cells, which are $z = 0$ half planes with $y > 0$ and $y < 0$, and two 1-cells, which are $z = y = 0$ half lines with $x > 0$ and $x < 0$. Last, the single 0-cell is the point at the origin.

As a second example, we took G_c to be space group #1, which consists only of translation symmetry. We set the lattice constant to unity and take the three Bravais lattice basis vectors to be (1,0,0), (0,1,0), and (0,0,1). A natural choice for an AU is simply the interior of a unit cell, i.e., the region $0 < x, y, z < 1$. The 3-cells are then the copies of the AU under translation. There are three kinds of 2-cells. One type consists of the xy plane (i.e., $z = 0$ plane) region with $0 < x, y < 1$ and its images under translation, and the other two types are similar but lie in the xz and yz planes. Similarly, there are three kinds of 1-cells, with one type consisting of the $x = y = 0$ region with $0 < z < 1$ and its images under translation. The other two types are similar regions

oriented along the x and y axes. Last, the 0-cells are points (n_x, n_y, n_z), with n_x, n_y, and n_z integers.

Formal structure of classification resolved by block dimension

Here, we describe the Abelian group structure of TCIs (32) and how taking a certain quotient allows us to ignore distinctions among atomic insulators. We let $\mathcal{D}_{d_b}$ be the Abelian group classifying insulators whose nontrivial building blocks are dimension d_b and below. That is, states classified by $\mathcal{D}_{d_b}$ can be reduced to a state on X^2 where all n-cells with $n > d_b$ host a trivial state. Clearly, $d_b = 0, 1$, and 2, and we have the sequence of subgroups $\mathcal{D}_0 \subset \mathcal{D}_1 \subset \mathcal{D}_2$. $\mathcal{D}_2$ as the classification of all TCIs or, at least, all those that can be classified in terms of topological crystals. The observation that all 1-cells are trivial implies that $\mathcal{D}_0 = \mathcal{D}_1$. Phases in $\mathcal{D}_0$ are atomic insulators, which we wish to exclude from consideration. Although there are distinct atomic insulators constituting different quantum phases of matter, all atomic insulators are, in some sense, topologically trivial. We can eliminate these states by taking the quotient $\mathcal{C} = \mathcal{D}_2/\mathcal{D}_0$, which gives the desired classification of TCIs.

Gluing MCI building blocks: Planar decomposition of MTCIs

Here, we address the consequences of the gluing conditions for MTCIs, i.e., topological crystals built from MCI building blocks placed on the 2-cells of X^2. In particular, we show that MTCIs can always be decomposed into decoupled planar MCI states placed on mirror planes. We consider a mirror plane P, and note that we must have $P \subset X^2$. Therefore, up to a set of measure zero, P is a union of 2-cells of X^2. We consider a 2-cell $e_1^2 \subset P$ and place an MCI state on e_1^2, whose invariant is some element of $\mathbb{Z}$. We want to show that symmetry and gluing along 1-cells imply that every 2-cell in P is an MCI with the same $\mathbb{Z}$ invariant as the state in e_1^2. It is enough to show that this holds for a single 2-cell $e_2^2 \subset P$ that is adjacent to e_1^2 in P. That is, e_1^2 and e_2^2 meet at a 1-cell $e^1 \subset P$, as illustrated in fig. S1.

To proceed, we consider a number of cases. In case (1), there exists an element $g \in G_c$ that maps e_1^2 to e_2^2. First, we show that symmetry requires that both 2-cells host an MCI state with the same invariant (this is not a priori obvious; it is conceivable that some symmetry operations could change the sign of the invariant). To begin, we claim that either $g\sigma = \sigma g$, when g preserves the orientation of the mirror plane, or $g\sigma = (-1)^F \sigma g$, when g reverses the orientation of the mirror plane. If we ignore factors of fermion parity, then $g\sigma = \sigma g$ or, equivalently, $g\sigma g^{-1} = \sigma$. To see this, we observe that $g \in G_P$, where G_P $_{G_c}$ is the group of symmetries of the mirror plane. Moreover, σ is the only nontrivial element of G_P that acts on the mirror plane as the identity rigid motion. The operation $g\sigma g^{-1}$ also acts on the mirror plane as the identity rigid motion, and σ cannot be conjugate to the identity in G_P; therefore, $g\sigma g^{-1} = \sigma$.

The relativistic Dirac Hamiltonian as discussed in the Supplementary Materials allows us to determine the presence or absence

of the $(-1)^F$ factor. We choose coordinates so that the mirror plane is the $z = 0$ plane, and the action of σ on the Dirac field $\Psi(\mathbf{r})$ is given in the Supplementary Materials. We consider a symmetry operation g that takes the mirror plane into itself, with action on the Dirac field

$$g : \Psi(\mathbf{r}) \rightarrow M_g \Psi(\mathbf{r}') \tag{3}$$

where

$$\mathbf{r}' = O\mathbf{r} + \vec{t} \tag{4}$$

where O is an orthogonal matrix. The requirement that the mirror plane goes into itself under g implies that $t_z = O_{zx} = O_{zy} = 0$. Moreover, because O is an orthogonal matrix, $O_{xz} = O_{yz} = 0$ and $O_{zz} = \pm 1$. We are free to multiply g by inversion and/or translations within the $z = 0$ plane to make g into a rotation. This can be done because both translations and inversion preserve the orientation of the $z = 0$ plane. Moreover, translations have no effect on M_g, while inversion commutes with σ. After doing this, there are two possibilities for g. One possibility is a rotation by θ with axis normal to the plane; this operation preserves the orientation of the plane, and we have $M_g = \exp(i\theta\mu^3/2)$ so that g commutes with σ. The other possibility is a C_2 rotation with axis normal to the plane; this operation reverses the orientation of the plane and anticommutes with σ. This establishes the claim that $g\sigma = \sigma g$, when g preserves the orientation of the mirror plane, or $g\sigma = (-1)^F \sigma g$, when g reverses the orientation of the mirror plane.

Now we use this claim to show that the MCI states on e_1^2 and e_2^2 have the same $\mathbb{Z}$ invariant. Consider a one-electron state $|\psi\rangle$ supported only on e_1^2, whose mirror eigenvalue is given by $\sigma | \psi \rangle = i | \psi \rangle$. The state $g | \psi\rangle$ is supported on e_2^2 and has mirror eigenvalue $+i$ if g preserves the orientation of the plane, and $-i$ if it reverses the orientation of the plane. Because the Chern number of each sector with fixed mirror eigenvalue is preserved when g preserves orientation and reversed when g reverses orientation, it follows that the two MCI states have the same $\mathbb{Z}$ index.

To complete the discussion of case (1), we need to address gluing of the two MCI states at e_1. It is enough to consider only symmetries that take the set of cells $\{e^1, e_1^2, e_2^2\}$ into itself. There are two subcases. In case (1a), the only relevant symmetry is the mirror reflection itself. In this case, it is obvious that two MCI states with the same invariant can be glued together along e^1. In case (1b), e^1 is contained within a C_{2v} axis. To analyze gluing at e^1, we studied the edge theory at e^1 for MCI states on e_1^2 and e_2^2. The edge of e_1^2 (e_2^2) consists of a pair of counterpropagating fermion modes c_{R1} and c_{L1} (c_{R2} and c_{L2}). We assemble these 1D fermions into the four-component field $\psi^T = (c_{R1}\ c_{L1}\ c_{R2}\ c_{L2})$. Denoting by σ' the mirror symmetry exchanging the two 2-cells, we take the symmetries to act by

$$T : \psi \rightarrow (i\mu^2)\psi \tag{5}$$

$$\sigma : \psi \rightarrow i\mu^3\tau^3\psi \tag{6}$$

$$\sigma' : \psi \rightarrow i\mu^3\tau^1\psi \tag{7}$$

where the μ^i and τ^i Pauli matrices act in the 4×4 matrix space just as in the earlier discussion of the relativistic Dirac Hamiltonian. These symmetries act appropriately on fermions and are compatible with the two 2-cells having the same MCI index. These symmetries allow the mass term $\psi^\dagger\mu^2\tau^2\psi$, which gaps out the fermions on e^1 and thus glues the two 2-cells together.

Now, we move on to case (2), where there is no element $g \in G_c$ that maps e_1^2 into e_2^2. In this case, symmetry does not determine which state is placed on e_2^2, but we will see that this is determined by gluing at e^1. We found it useful to consider the 3-cells that meet at e_1^2 and e_2^2. These are defined in fig. S2. We considered two subcases. In case (2a), $e_{1\uparrow}^2 = e_{2\uparrow}^2$. It follows immediately that $e_{1\downarrow}^2 = e_{2\downarrow}^2$, so there is only a single 3-cell above and below the mirror plane in the region shown in fig. S2. This means that e_1^2 and e_2^2 are the only 2-cells meeting at e^1, which further implies that the only symmetry taking e^1 into itself is the mirror symmetry. The gluing condition at e^1 is then satisfied if and only if an MCI state is placed in e_2^2.

In case (2b), $e_{1\uparrow}^2 \neq e_{2\uparrow}^2$, which implies that e_1^2 and e_2^2 are not the only 2-cells meeting at e^1. The additional 2-cells come in mirror-symmetric pairs above and below the mirror plane. There are two further subcases. In case (2b.i), the only symmetry taking e^1 into itself is the mirror symmetry. In this case, the additional pairs of 2-cells do not coincide with mirror planes. Therefore, for each pair, the only nontrivial possibility is that both 2-cells host a 2dTI state, in which case the 2dTI edges of the pair can be gapped out at e^1. The relevant edge theory for each pair at e^1 is the same as that discussed in case (1), except with only σ' and T symmetry (i.e., without σ symmetry), and it follows from the discussion there that this edge can be gapped. Therefore, these additional pairs of 2-cells can be effectively eliminated, and the gluing condition again requires us to place an MCI state on e_2^2.

Last, in case (2b.ii), e^1 is contained in a C_{3v} axis, where the C_{3v} symmetry is generated by σ and a 3-fold rotation C_3. Here, there are six 2-cells that coincide with the mirror planes meeting at e^1. These 2-cells come in three pairs, with each pair contained in one of the three mirror planes that intersect e^1. e_1^2 and e_2^2 constitute one such pair, with the other two pairs obtained from it under the 3-fold rotation. We suppose that an MCI state is placed on e_1^2 and its rotation images, but not on e_2^2 (see fig. S3); we show that it is impossible to gap out the resulting edge theory at e^1, which imply that, again, an MCI state must be placed on e_2^2. The edge fermions for the e_1^2 MCI are c_{R1} and c_{L1}, with

$$\sigma : \begin{cases} c_{R1} \rightarrow i c_{R1} \\ c_{L1} \rightarrow -i c_{L1} \end{cases} \tag{8}$$

The images of these fermions under C_3 rotation are $c_{R2} = C_3 c_{R1} C_3^{-1}$ and $c_{R3} = C_3^2 c_{R1} C_3^{-2}$, with identical expressions holding for the left-moving modes. The generators of the C_{3v} group satisfy the following relations, acting on a fermion field

$$\sigma^2 = -1 \tag{9}$$

$$C_3^3 = -1 \tag{10}$$

$$(\sigma C_3)^2 = -1 \tag{11}$$

Using these relations, we find

$$\sigma : \begin{cases} c_{R2} \rightarrow -ic_{R3} \\ c_{L2} \rightarrow ic_{L3} \\ c_{R3} \rightarrow -ic_{R2} \\ c_{L3} \rightarrow ic_{L2} \end{cases} \tag{12}$$

Now, focusing only on the mirror reflection symmetry, we can change variables to diagonalize σ and find that the c_{R2}, c_{R3}, c_{L2}, and c_{L3} fermion modes can be gapped out. This leaves the c_{R1} and c_{L1} edge of the MCI state on e_1^2, which cannot be gapped; this establishes the desired result.

Gluing condition for $\mathbb{Z}_2$ TCIs

Here, we consider the gluing condition for $\mathbb{Z}_2$ TCIs, i.e., the requirement that there are no gapless modes within the bulk. If we consider placing 2dTI states on a subset of the 2-cells of X^2, then we will show that the gluing condition can be satisfied if and only if an even number of 2dTI edges meet at each 1-cell. This is illustrated in fig. S4 for the space groups $P3$ (no. 143) and $P4$ (no. 75). One direction is trivial to show: If the gluing condition is satisfied, then an even number of 2dTI edges must meet at each 1-cell e^1 because, otherwise, time reversal would forbid e^1 from being gapped.

Now, we suppose that we place 2dTI states on 2-cells of X^2 such that an even number of 2dTI edges meets at each 1-cell. We would like to show that each 1-cell can be gapped; thus, the gluing condition is satisfied. We do this by considering the different possible point group symmetries of a 1-cell e^1, which may impose constraints on gluing of 2dTI edge modes along e^1. If e^1 has trivial point group symmetry, then the only symmetries are charge conservation and time reversal, and an even number of 2dTI edge modes can always be gapped. If e^1 is contained in a mirror plane, then 2dTI edge modes come in mirror-symmetric pairs above and below the mirror plane, and we have already shown in the above that each such pair can be gapped.

Next, we consider the case where e^1 is contained in a C_n axis. When $n = 2$, 2dTI edge modes come in pairs related by C_2 symmetry, and the action of C_2 symmetry on such a pair is identical to that of the σ' symmetry discussed above (see Eq. 7 and the surrounding discussion). Therefore, these pairs of edge modes can be gapped. When $n > 2$ is even, edge modes come in groups of n related by C_n symmetry, and these can be grouped into $n/2$ pairs related by C_2 symmetry. We can focus on one such pair and gap it out, then use the C_n symmetry to "copy" its mass term to the other $n/2 - 1$ pairs, which gaps out all the modes respecting the C_n symmetry. Last, for C_3 symmetry, edge modes must come in groups of six, with two sets of three edge modes related by symmetry. We can take a pair of edge modes unrelated by symmetry and gap these out and then use the C_3 symmetry to copy the resulting mass term to the other two pairs of edge modes.

Similar arguments can be applied when e^1 is contained in a C_{nv} axis. Here, 2-cells that can host 2dTIs lie away from the mirror planes, so that edge modes come in groups of $2n$ related by C_{nv} symmetry. Viewing C_{nv} as generated by a mirror reflection and C_n rotation, we can start by gapping out a pair of neighboring edge modes related by the mirror symmetry and then copying its mass term using the rotational symmetry.

Gluing at 0-cells

In the analysis of the gluing condition in the above, we started with a set of topological states on 2-cells and considered gluing these states

together at 1-cells. In principle, this may not be the end of the story; we needed to consider gluing at 0-cells. That is, we needed to ensure that there are no localized protected gapless states at 0-cells, which would violate the gluing condition. However, there is a simple reason this cannot occur: consider the set of gapped 1-cells that meet at a 0-cell. We can lump these 1-cells together and view them as a single gapped $d = 1$ system, with the 0-cell as its endpoint. Upon decomposing the spectrum into irreducible representations of any site symmetry at the 0-cell, this $d = 1$ system divides into sectors that are either in class A or AII. To have a protected gapless state on the 0-cell, the $d = 1$ system would need to be topologically nontrivial, but class A and AII have a trivial classification in $d = 1$.

Nontrivial example of equivalence operation

In the Results section, we discussed an equivalence operation involving creating bubbles of 2dTI within each AU, which turns out to have a trivial effect on the classification of time-reversal symmetric electronic TCIs. To clarify the nature and role of this equivalence operation, here we discuss an example without time-reversal symmetry where it does modify the classification. We consider $d = 3$ insulators without time-reversal symmetry with point group $\bar{1}$. Ignoring the inversion symmetry, this is a system in symmetry class A. We choose the 2-skeleton X^2 as the $z = 0$ plane, the 1-skeleton X^1 as the $z = y = 0$ line, and the 0-skeleton X^0 as the point at the origin, as shown in Fig. 4A. Phases constructed by decorating X^0 with $d_b = 0$ building blocks are atomic insulators, which are excluded from consideration; thus, we need only to consider X^1 and X^2. The only internal symmetry on X^1 and X^2 is the charge conservation, which protects a $\mathbb{Z}$-classification in $d = 2$, corresponding to Chern insulators, and a trivial classification in $d = 1$. Thus, to obtain the TCI classification, we only need to consider topological crystals obtained by decorating X^2 with Chern insulators.

First, we consider the gluing condition on X^2. X^2 decompose into two 2-cells: $e_1^2 : z = 0, x > 0, e_2^2 : z = 0, x < 0$. We decorate e_1^2 with a Chern insulator with Chern number $C (\in \mathbb{Z})$ and e_2^2 with a symmetric copy of this Chern insulator under inversion. Since chirality remains unchanged under inversion, this copy has the identical Chern number C, and the chiral boundary states of e_1^2 and e_2^2 cancel each other on the 1-skeleton X^1. Therefore, the gluing condition allows a $\mathbb{Z}$ classification on X^2.

We now consider the equivalence operation. We create a bubble of Chern insulator with Chern number 1 in the $z > 0$ region. Because
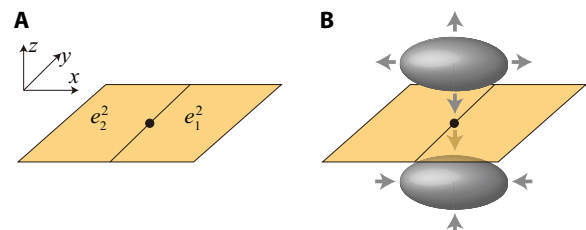

Fig. 4. Illustration of the effects of the equivalence operation in point group $\bar{1}$ without time-reversal symmetry. (**A**) The 2-cells: $e_1^2 : z = 0, x > 0$ and $e_2^2 : z = 0, x < 0$. (**B**) The equivalence operation. When a bubble made of 2D Chern insulator with Chern number 1 is created in $z > 0$, another Chern bubble with Chern number -1 in $z < 0$ will be created because of the inversion symmetry. The arrows represent the orientation of the Chern number. We enlarge these two bubbles until they join with the $z = 0$ plane; then, the Chern number of the state on $z = 0$ will be subducted by 2.

of the inversion symmetry, another bubble will be created in the $z < 0$ region as shown in Fig. 4B. We enlarge the two bubbles respecting the inversion symmetry, until the bottom surface of the $z > 0$ bubble joins with X^2 and the rest of the bubble moves to infinity. At the same time, the top surface of the $z < 0$ bubble also joins with X^2. Therefore, after this operation, the total Chern number on X^2 is increased by 2, which implies that the classification is reduced from $\mathbb{Z}$ to $\mathbb{Z}_2$.

This class A $\mathbb{Z}_2$ TCI has been discussed in (21, 47, 48).

Topological crystals, topological invariants, and $H^1(G, \mathbb{Z}_2)$

In this section, we give a more detailed discussion of the $\mathbb{Z}_2$-valued function of invariants $\delta(g)$ characterizing a topological crystal. On the basis of this discussion, we established a connection between the classification $\mathcal{C}$ of TCIs and $H^1(G_c, \mathbb{Z}_2)$, which allows $\mathcal{C}$ to be computed with the aid of standard computer algebra tools such as GAP (49). In particular, we show that $\mathcal{C}$ and $H^1(G_c, \mathbb{Z}_2)$ have the same number of generators.

In the text, we defined $\delta(g)$ only for a $\mathbb{Z}_2$ TCI. It will be useful for our present purposes to give a definition valid for an arbitrary topological crystal. First, we introduce the notion of a $\mathbb{Z}_2$ coloring of X^2, which is given by associating a $\mathbb{Z}_2$ number to each 2-cell of X^2 so that each 2-cell is either colored and assigned 1, or empty and assigned 0. These $\mathbb{Z}_2$ numbers must be assigned to respect the crystalline symmetry and satisfy a gluing condition, namely, for each 1-cell, an even number of the 2-cells meeting there must be colored. $\mathbb{Z}_2$ colorings can be added using the $\mathbb{Z}_2$ addition law, and this makes $\mathbb{Z}_2$ colorings into a group that we denote by $\tilde{\mathcal{C}}$ [we remark that $\mathbb{Z}_2$ colorings can be viewed as elements of the homology group $H_2(X^2; \mathbb{Z}_2)$ satisfying a symmetry condition, but we will not make use of this here.]

Next, we observe that there is a map from topological crystals (elements of $\mathcal{C}$) to $\tilde{\mathcal{C}}$. We denote this map by $\pi : \mathcal{C} \to \tilde{\mathcal{C}}$. Empty cells of the topological crystal map to empty cells in the $\mathbb{Z}_2$ coloring. Cells decorated with 2dTI map to colored cells. Cells decorated with an MCI state map to colored cells when the mirror Chern number is odd and to empty cells when it is even (we used the convention that the smallest possible mirror Chern number is 1; some authors use a definition of mirror Chern number that is twice our definition).

Last, given a $\mathbb{Z}_2$ coloring of X^2, we define $\delta(g)$ as in the Results section. That is, we arbitrarily choose one AU, let $\mathbf{r}$ be a point inside, and define $\delta(g) = 1$ if a path connecting $\mathbf{r}$ to $g\mathbf{r}$ crosses an odd number of colored 2-cells, while $\delta(g) = 0$ if the path crosses an even number of colored 2-cells. The path should be chosen to avoid 0-cells and 1-cells but is otherwise an arbitrary continuous path.

We now establish some properties of $\delta(g)$ quoted in the Results section. First, we show that $\delta(g)$ is independent of the path chosen to connect $\mathbf{r}$ to $g\mathbf{r}$ and is, thus, a well-defined function mapping G_c to $\mathbb{Z}_2$. Any two such paths are related by a finite number of moves, where a segment of the path is passed through a 1-cell. The gluing condition says that an even number of colored 2-cells meet at every 1-cell, so these moves do not affect $\delta(g)$. At this stage, we have not yet shown that δ is independent of the arbitrary choice of AU.

Next, we show that δ is a homomorphism from G_c to $\mathbb{Z}_2$, that is, $\delta(g_1 g_2) = \delta(g_1) + \delta(g_2)$. We compute $\delta(g_1 g_2)$ by considering a path from $\mathbf{r}$ to $g_1 g_2 \mathbf{r}$ that first goes from $\mathbf{r}$ to $g_1 \mathbf{r}$ and then goes from $g_1 \mathbf{r}$ to $g_1 g_2 \mathbf{r}$. The number of colored 2-cells modulo 2 crossed by the first segment is $\delta(g_1)$ by definition. The second segment is related by symmetry to a path joining $\mathbf{r}$ to $g_2 \mathbf{r}$, so $\delta(g_2)$ is the number of colored 2-cells (modulo 2) crossed by the second segment. Therefore, $\delta(g_1 g_2) = \delta(g_1) + \delta(g_2)$.

Last, we show that δ does not depend on the arbitrary choice of AU. Let $\delta(g)$ be the function defined by choosing an AU with a point $\mathbf{r}$ inside, and let $\delta'(g)$ be the function defined by choosing a different AU, which contains a point $g_0 \mathbf{r}$ for some $g_0 \in G_c$. Then, $\delta'(g)$ is the number of colored 2-cells (modulo 2) crossed by a path connecting $g_0 \mathbf{r}$ to $g g_0 \mathbf{r}$. By symmetry, this number is the same as for a path joining $\mathbf{r}$ to $g_0^{-1} g g_0 \mathbf{r}$, which shows that $\delta'(g) = \delta(g_0^{-1} g g_0)$. But this implies that $\delta'(g) = \delta(g)$ because δ is a homomorphism and $\mathbb{Z}_2$ is Abelian.

Our construction of δ gives a map $\Delta : \tilde{\mathcal{C}} \to H^1(G_c, \mathbb{Z}_2)$, where $H^1(G_c, \mathbb{Z}_2)$ is viewed as the group of homomorphisms from G_c to $\mathbb{Z}_2$. Δ is an isomorphism, so $\tilde{\mathcal{C}} \simeq H^1(G_c, \mathbb{Z}_2)$. It is easy to see that Δ is injective. To see that Δ is surjective, we need to show that given $\delta : G_c \to \mathbb{Z}_2$, we can construct a corresponding $\mathbb{Z}_2$ coloring. Upon arbitrarily choosing an AU, the 3-cells of $\mathbb{R}^3$ are in one-to-one correspondence with elements of G_c. We then color each 3-cell with the $\mathbb{Z}_2$ number $\delta(g)$. Given a 2-cell, let g_1 and g_2 label the two 3-cells that meet at the 2-cell. We then color the 2-cell with the $\mathbb{Z}_2$ number $\delta(g_1) + \delta(g_2)$. The resulting assignment of $\mathbb{Z}_2$ numbers to 2-cells is clearly symmetric and satisfies the gluing condition and is, thus, a $\mathbb{Z}_2$ coloring of X^2. By construction, Δ maps this $\mathbb{Z}_2$ coloring to δ.

Now that we have shown that $\tilde{\mathcal{C}} \simeq H^1(G_c, \mathbb{Z}_2)$, we would like to show that $\mathcal{C}$ and $\tilde{\mathcal{C}}$ have the same number of generators. First, we observed that $\mathcal{C} = \mathcal{C}_{\mathrm{MCI}} \times \mathcal{C}_{2dTI}$, where $\mathcal{C}_{\mathrm{MCI}}$ is the classification of MTCIs (i.e., topological crystals built from MCI states) and $\mathcal{C}_{2dTI}$ is the classification of $\mathbb{Z}_2$ TCIs. $\mathcal{C}_{\mathrm{MCI}}$ is a product of $\mathbb{Z}$ factors, and $\mathcal{C}_{2dTI}$ is a product of $\mathbb{Z}_2$ factors. We introduce a similar decomposition $\tilde{\mathcal{C}} = \tilde{\mathcal{C}}_{\mathrm{MCI}} \times \tilde{\mathcal{C}}_{2dTI}$, where $\tilde{\mathcal{C}}_{\mathrm{MCI}}$ is defined to be the subgroup of $\mathbb{Z}_2$ colorings whose colored 2-cells lie in mirror planes, and $\tilde{\mathcal{C}}_{2dTI}$ is the subgroup of $\mathbb{Z}_2$ colorings where all 2-cells lying in mirror planes are empty. Clearly $\tilde{\mathcal{C}}$, $\tilde{\mathcal{C}}_{\mathrm{MCI}}$, and $\tilde{\mathcal{C}}_{2dTI}$ are all products of $\mathbb{Z}_2$ factors. To prove that $\tilde{\mathcal{C}} = \tilde{\mathcal{C}}_{\mathrm{MCI}} \times \tilde{\mathcal{C}}_{2dTI}$, it is enough to show that an arbitrary $\mathbb{Z}_2$ coloring $c \in \tilde{\mathcal{C}}$ can be written uniquely as $c = c_m c_{\bar{m}}$ for some $c_m \in \tilde{\mathcal{C}}_{\mathrm{MCI}}$ and $c_{\bar{m}} \in \tilde{\mathcal{C}}_{2dTI}$. Given $c \in \tilde{\mathcal{C}}$, we consider a 1-cell e^1 contained in a mirror plane. n 2-cells meet at e^1, two of which lie in the mirror plane, and $n - 2$ of which lie outside the mirror plane. The $n - 2$ 2-cells outside the mirror plane can be grouped into pairs related by mirror reflection, so that the two 2-cells in each pair are either both colored or both empty. It follows that the two 2-cells contained in the mirror plane are also either both colored or both empty. Therefore, we define a new $\mathbb{Z}_2$ coloring $c_m \in \tilde{\mathcal{C}}_{\mathrm{MCI}}$ by starting with c and replacing all colored 2-cells not lying in mirror planes with empty cells. Similarly, if we replace all the colored 2-cells within mirror planes with empty cells, then we obtain $c_{\bar{m}} \in \tilde{\mathcal{C}}_{2dTI}$. It is obvious that $c = c_m c_{\bar{m}}$ and that c_m and $c_{\bar{m}}$ are unique.

Using the above discussion, we showed that the map $\pi : \mathcal{C} \to \tilde{\mathcal{C}}$ gives a one-to-one correspondence between generators of $\mathcal{C}$ and $\tilde{\mathcal{C}}$, so the two groups have the same number of generators. First, restricting π to $\mathcal{C}_{2dTI}$ gives an isomorphism between $\mathcal{C}_{2dTI}$ and $\tilde{\mathcal{C}}_{2dTI}$, so these subgroups clearly have the same number of generators. Second, we can take each $\mathbb{Z}$ factor of $\mathcal{C}_{\mathrm{MCI}}$ to be generated from a topological crystal obtained by decorating the 2-cells of a mirror plane, as well as all symmetry-equivalent mirror planes, with an MCI state of unit Chern number. The above discussion implies that $\tilde{\mathcal{C}}_{\mathrm{MCI}}$ is generated by $\mathbb{Z}_2$ colorings obtained by coloring all the 2-cells of set of symmetry-equivalent mirror planes, and these generators are images of the $\mathcal{C}_{\mathrm{MCI}}$ generators under π, giving a one-to-one correspondence between generators of $\mathcal{C}_{\mathrm{MCI}}$ and $\tilde{\mathcal{C}}_{2dTI}$.

These results make it a simple matter to compute the TCI classification $\mathcal{C}$. First, we compute $H^1(G_c, \mathbb{Z}_2)$; this can be done using GAP

(49). Then, we know that the number of $\mathbb{Z}$ factors in $\mathcal{C}$ is n_M, the number of symmetry-inequivalent sets of mirror planes. We then obtain $\mathcal{C}$ from $H^1(G_c, \mathbb{Z}_2)$ by replacing n_M of the $\mathbb{Z}_2$ factors with $\mathbb{Z}$ factors. For a G_c crystallographic point group or space group, n_M can be obtained immediately from information tabulated in the International Tables for Crystallography (50). The results of this procedure are presented in Table 1 for crystalline point groups, and in Table 2 for space groups. As discussed in the Introduction, we note that Khalaf et al. (36) have also obtained the results in these tables via a mathematically equivalent procedure.

While useful, we emphasize that this largely automated procedure is not a substitute for explicit real-space construction of topological crystals for a given symmetry group of interest, as described in Results. The latter procedure not only results in the same group structure but also provides additional physical insight and a starting point for further analysis, by giving an explicit real-space construction of each of the TCI phases classified. We also obtained the results in Table 2 by automating the explicit real-space constructions.

SUPPLEMENTARY MATERIALS

Fig. S1. Illustration of the 2-cells e_1^2 and e_2^2 and the 1-cell e^1 used to discuss the effect of gluing conditions on MTCIs.
Fig. S2. The 3-cells $e_{1\uparrow}^3$ and $e_{1\downarrow}^3$ ($e_{2\uparrow}^3$ and $e_{2\downarrow}^3$) meet at the 2-cell e_1^2 (e_2^2).
Fig. S3. Cross section through e^1 and the 2-cells that meet at e^1, in case (2b.ii), where e^1 is contained in a C_{3v} axis.
Fig. S4. Illustration of the effects of the gluing condition for $\mathbb{Z}_2$ TCIs for two representative space groups.
Table S1. Topological crystals beyond layer construction.
Table S2. Classification $\mathcal{C}_{\text{full}}$ of STIs and TCIs with time-reversal symmetry and spin-orbital coupling for all point groups.
Table S3. Classification $\mathcal{C}_{\text{full}}$ of STIs and TCIs with time-reversal symmetry and spin-orbital coupling for all space groups.

REFERENCES AND NOTES

1. T. Senthil, Symmetry-protected topological phases of quantum matter. *Annu. Rev. Condens. Matter Phys.* **6**, 299–324 (2015).
2. A. P. Schnyder, S. Ryu, A. Furusaki, A. W. W. Ludwig, Classification of topological insulators and superconductors in three spatial dimensions. *Phys. Rev. B* **78**, 195125 (2008).
3. A. Kitaev, *AIP Conf. Proc.* **1134**, 22 (2009).
4. S. Ryu, A. P. Schnyder, A. Furusaki, A. W. W. Ludwig, Topological insulators and superconductors: Tenfold way and dimensional hierarchy. *New J. Phys.* **12**, 065010 (2010).
5. C.-K. Chiu, J. C. Y. Teo, A. P. Schnyder, S. Ryu, Classification of topological quantum matter with symmetries. *Rev. Mod. Phys.* **88**, 035005 (2016).
6. L. Fu, Topological crystalline insulators. *Phys. Rev. Lett.* **106**, 106802 (2011).
7. T. H. Hsieh, H. Lin, J. Liu, W. Duan, A. Bansil, Topological crystalline insulators in the SnTe material class. *Nat. Commun.* **3**, 982 (2012).
8. Y. Ando, L. Fu, Topological crystalline insulators and topological superconductors: From concepts to materials. *Annu. Rev. Condens. Matter Phys.* **6**, 361–381 (2015).
9. P. Dziawa, B. J. Kowalski, K. Dybko, R. Buczko, A. Szczerbakow, M. Szot, E. Łusakowska, T. Balasubramanian, B. M. Wojek, M. H. Berntsen, O. Tjernberg, T. Story, Topological crystalline insulator states in Pb$_{1-x}$Sn$_x$Se. *Nat. Mater.* **11**, 1023–1027 (2012).
10. Y. Tanaka, Z. Ren, T. Sato, K. Nakayama, S. Souma, T. Takahashi, K. Segawa, Y. Ando, Experimental realization of a topological crystalline insulator in SnTe. *Nat. Phys.* **8**, 800–803 (2012).
11. S.-Y. Xu, C. Liu, N. Alidoust, M. Neupane, D. Qian, I. Belopolski, J. D. Denlinger, Y. J. Wang, H. Lin, L. A. Wray, G. Landolt, B. Slomski, J. H. Dil, A. Marcinkova, E. Morosan, Q. Gibson, R. Sankar, F. C. Chou, R. J. Cava, A. Bansil, M. Z. Hasan, Observation of a topological crystalline insulator phase and topological phase transition in Pb$_{1-x}$Sn$_x$Te. *Nat. Commun.* **3**, 1192 (2012).
12. C.-K. Chiu, H. Yao, S. Ryu, Classification of topological insulators and superconductors in the presence of reflection symmetry. *Phys. Rev. B* **88**, 075142 (2013).
13. G. Yang, J. Liu, L. Fu, W. Duan, C. Liu, Weak topological insulators in PbTe/SnTe superlattices. *Phys. Rev. B* **89**, 085312 (2014).
14. K. Shiozaki, M. Sato, Topology of crystalline insulators and superconductors. *Phys. Rev. B* **90**, 165114 (2014).
15. C. Fang, L. Fu, New classes of three-dimensional topological crystalline insulators: Nonsymmorphic and magnetic. *Phys. Rev. B* **91**, 161105 (2015).
16. K. Shiozaki, M. Sato, K. Gomi, Z2 topology in nonsymmorphic crystalline insulators: Möbius twist in surface states. *Phys. Rev. B* **91**, 155120 (2015).
17. K. Shiozaki, M. Sato, K. Gomi, *Phys. Rev. B* **93**, 195413 (2016).
18. Z. Wang, A. Alexandradinata, R. J. Cava, B. A. Bernevig, Hourglass fermions. *Nature* **532**, 189–194 (2016).
19. B. Bradlyn, L. Elcoro, J. Cano, M. G. Vergniory, Z. Wang, C. Felser, M. I. Aroyo, B. A. Bernevig, Topological quantum chemistry. *Nature* **547**, 298–305 (2017).
20. H. C. Po, A. Vishwanath, H. Watanabe, Symmetry-based indicators of band topology in the 230 space groups. *Nat. Commun.* **8**, 50 (2017).
21. C. Fang, L. Fu, Rotation anomaly and topological crystalline insulators. arXiv:1709.01929 (2017).
22. J. Kruthoff, J. de Boer, J. van Wezel, C. L. Kane, R.-J. Slager, Topological classification of crystalline insulators through band structure combinatorics. *Phys. Rev. X* **7**, 041069 (2017).
23. B. J. Wieder, B. Bradlyn, Z. Wang, J. Cano, Y. Kim, H.-S. D. Kim, A. M. Rappe, C. L. Kane, B. A. Bernevig, Wallpaper fermions and the nonsymmorphic Dirac insulator. *Science* **361**, 246 (2018).
24. C. Z. Xiong, A. Alexandradinata, Organizing symmetry-protected topological phases by layering and symmetry reduction: A minimalist perspective. *Phys. Rev. B* **97**, 115153 (2018).
25. Y. Okada, M. Serbyn, H. Lin, D. Walkup, W. Zhou, C. Dhital, M. Neupane, S. Xu, Y. J. Wang, R. Sankar, F. Chou, A. Bansil, M. Z. Hasan, S. D. Wilson, L. Fu, V. Madhavan, Observation of Dirac node formation and mass acquisition in a topological crystalline insulator. *Science* **341**, 1496–1499 (2013).
26. P. Sessi, D. Di Sante, A. Szczerbakow, F. Glott, S. Wilfert, H. Schmidt, T. Bathon, P. Dziawa, M. Greiter, T. Neupert, G. Sangiovanni, T. Story, R. Thomale, M. Bode, Robust spin-polarized midgap states at step edges of topological crystalline insulators. *Science* **354**, 1269–1273 (2016).
27. J. Ma, F. Wang, S. A. Denisov, A. Adhikary, M. Mostafavi, Reactivity of prehydrated electrons toward nucleobases and nucleotides in aqueous solution. *Sci. Adv.* **3**, e1701669 (2017).
28. D. S. Freed, G. W. Moore, Twisted equivariant matter. *Ann. Henri Poincaré* **14**, 1927–2023 (2013).
29. H. Song, S.-J. Huang, L. Fu, M. Hermele, Topological phases protected by point group symmetry. *Phys. Rev. X* **7**, 011020 (2017).
30. S. Jiang, Y. Ran, Anyon condensation and a generic tensor-network construction for symmetry-protected topological phases. *Phys. Rev. B* **95**, 125107 (2017).
31. R. Thorngren, D. V. Else, Gauging spatial symmetries and the classification of topological crystalline phases. *Phys. Rev. X* **8**, 011040 (2018).
32. S.-J. Huang, H. Song, Y.-P. Huang, M. Hermele, Building crystalline topological phases from lower-dimensional states, *Phys. Rev. B* **96**, 205106 (2017).
33. B. Han, H. Wang, P. Ye, Generalized Wen-Zee terms. *Phys. Rev. B* **99**, 205120 (2019).
34. K. Shiozaki, C. Zhaoxi Xiong, K. Gomi, Generalized homology and Atiyah-Hirzebruch spectral sequence in crystalline symmetry protected topological phenomena. arXiv:1810.00801 (2018).
35. Z. Song, T. Zhang, Z. Fang, C. Fang, Quantitative mappings between symmetry and topology in solids. *Nat. Commun.* **9**, 3530 (2018).
36. E. Khalaf, H. C. Po, A. Vishwanath, H. Watanabe, Symmetry indicators and anomalous surface states of topological crystalline insulators. *Phys. Rev. X* **8**, 031070 (2018).
37. L. Fu, C. L. Kane, E. J. Mele, Topological insulators in three dimensions. *Phys. Rev. Lett.* **98**, 106803 (2007).
38. J. E. Moore, L. Balents, Topological invariants of time-reversal-invariant band structures. *Phys. Rev. B* **75**, 121306 (2007).
39. J. C. Y. Teo, L. Fu, C. L. Kane, Topological invariants of time-reversal-invariant band structures. *Phys. Rev. B* **78**, 045426 (2008).
40. Z. Song, Z. Fang, C. Fang, (d−2)-dimensional edge states of rotation symmetry protected topological states. *Phys. Rev. Lett.* **119**, 246402 (2017).
41. A. M. Turner, Y. Zhang, A. Vishwanath, Entanglement and inversion symmetry in topological insulators. *Phys. Rev. B* **82**, 241102 (2010).
42. T. L. Hughes, E. Prodan, B. A. Bernevig, Inversion-symmetric topological insulators. *Phys. Rev. B* **83**, 245132 (2011).
43. E. Cornfeld, A. Chapman, Classification of crystalline topological insulators and superconductors with point group symmetries. *Phys. Rev. B* **99**, 075105 (2019).
44. T. Morimoto, A. Furusaki, C. Mudry, Breakdown of the topological classification $\mathbb{Z}$ for gapped phases of noninteracting fermions by quartic interactions. *Phys. Rev. B* **92**, 125104 (2015).
45. Z. Song, T. Zhang, C. Fang, Diagnosis for nonmagnetic topological semimetals in the absence of spin-orbital coupling. *Phys. Rev. X* **8**, 031069 (2018).

46. A. Hatcher, *Algebraic Topology* (Cambridge Univ. Press, 2001).
47. M. Geier, L. Trifunovic, M. Hoskam, P. W. Brouwer, Second-order topological insulators and superconductors with an order-two crystalline symmetry. *Phys. Rev. B* **97**, 205135 (2018).
48. E. Khalaf, Higher-order topological insulators and superconductors protected by inversion symmetry. *Phys. Rev. B* **97**, 205136 (2018).
49. The GAP Group, *GAP—Groups, Algorithms, and Programming, Version 4.9.3* (2018).
50. T. Hahn, ed., *International Tables for Crystallography, Vol. A: Space-Group Symmetry* (Wiley, 2006).